Journal of Polymer Science

WILEY

JOURNAL OF POLYMER SCIENCE

PERSPECTIVE OPEN ACCESS

Fiber Processing of Recombinant Spider Silk Proteins

Manuel Michel[1] | Thomas Scheibel[1,2,3,4,5]

[1]Biomaterials, Engineering Faculty, University of Bayreuth, Bayreuth, Germany | [2]Bayreuth Center for Colloids and Interfaces (BZKG), University of Bayreuth, Bayreuth, Germany | [3]Bavarian Polymer Institute (BPI), University of Bayreuth, Bayreuth, Germany | [4]Bayreuth Center for Molecular Biosciences (BZMB), University of Bayreuth, Bayreuth, Germany | [5]Bayreuth Center for Material Science (BayMAT), University of Bayreuth, Bayreuth, Germany

Correspondence: Thomas Scheibel (thomas.scheibel@uni-bayreuth.de)

Received: 22 January 2025 | **Revised:** 27 March 2025 | **Accepted:** 3 April 2025

Keywords: biomimetic spinning | centrifugal spinning | electrospinning | hierarchical structures | Janus fibers | microfluidics | yarn spinning

ABSTRACT

Spider silks are protein-based fibers well known for their tensile strength, elasticity, and extraordinary toughness. However, spider silk has not yet been found to enter many products, since harvesting natural spider silk is highly inefficient. Recombinant production of the underlying spider silk proteins in microbial hosts offers an alternative to develop silk materials for distinct applications. In this context, it is crucial to mimic the spinning dope preparation and the spinning process of spiders to achieve nature-like fiber properties, since the mechanical properties of the fibers differ significantly depending on the utilized spinning method. In contrast, nonnatural spinning techniques facilitate the fabrication of silk fibers with tunable new properties for diverse technical applications. Electrospinning, for instance, produces fibers with diameters in the submicrometer regime, forming meshes ideal, e.g., for filtration. Centrifugal electrospinning increases fiber throughput, making it suitable for scale-up production. Even hierarchical structures can be created by combining 3D printing and centrifugal electrospinning within a single device, or yarn electrospinning combined with textile techniques, enabling complex architectures. This perspective article highlights how different spinning approaches broaden the potential uses of silk-based materials across various application fields, utilizing the benefits of intrinsic silk characteristics in combination with advanced technical features.

1 | Introduction

Fibers with high toughness can absorb tremendous amounts of energy before failure, ensuring durability and resilience. Interestingly, no natural or synthetic fiber used in modern engineering can match the outstanding toughness of certain spider silks, which is based on their intrinsic properties [1].

To effectively catch prey, a spider web not only relies on the strength of individual fibers but also on the architectural arrangement of these fibers into a cohesive, resilient network [2]. The web acts as a composite material, wherein various silk types are placed at specific locations to optimize energy absorption and impact resistance (Figure 1A) [3]. This design allows the web to absorb the impact of a flying insect and successfully stop it in full flight. In an orb web, up to five different silks are used, including one glue to prevent prey from escaping the web.

Studies have shown that the different silk types exhibit distinct molecular structures, yielding different mechanical properties. Key amino acid motifs in spider silk proteins drive the formation of secondary structures such as β-sheets, β-spirals, and α-helices, each contributing to the fibers' mechanical properties (Figure 1B) [3].

The best-investigated spider silk, major ampullate (MA), also known as dragline silk, is used to build the framework of the web by providing critical structural support, due to an exceptional combination of strength and extensibility [4]. On a molecular level, MA silk proteins (= MA spidroins, MaSp)

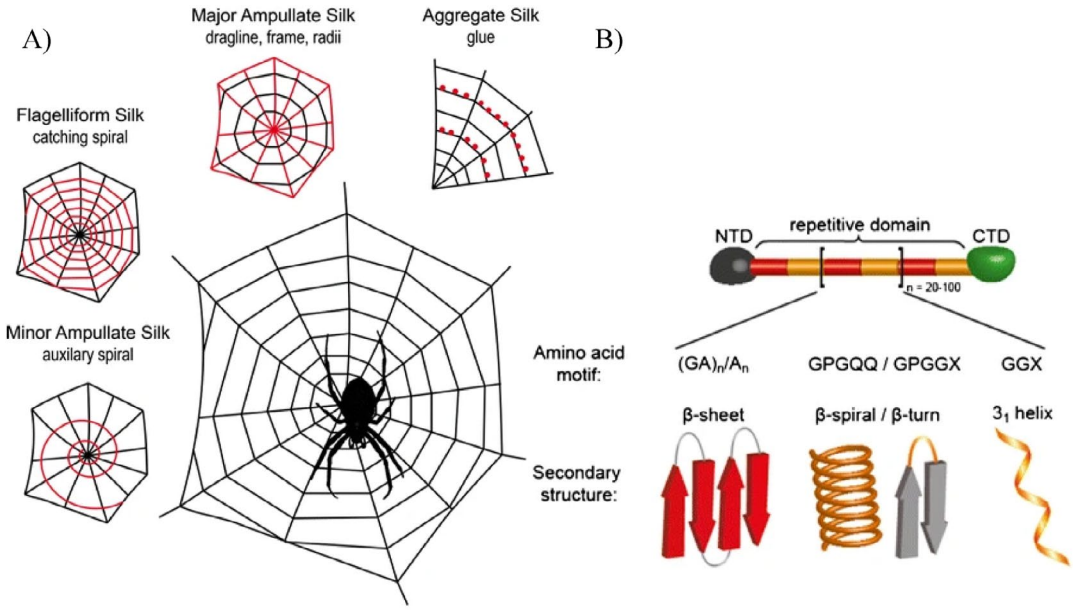

FIGURE 1 | Orb web and spider silk composition. (A) Illustrated representation of selected silk types produced by female orb-weaving spiders (Araneae), with each silk type marked in red to emphasize its unique function for specific tasks as indicated. (B) Molecular structure of major ampullate spidroins, highlighting the recurring amino acid motifs and their associated secondary structures. The symbol X represents predominantly tyrosine, leucine, glutamine, alanine, or serine residues. NTD denotes a nonrepetitive amino-terminal domain, and CTD denotes a nonrepetitive carboxyl-terminal domain. Adapted with permission from [3]. 2015, Springer Nature.

contain a high proportion of β-sheets creating crystalline regions responsible for strength, while amorphous regions ensure flexibility [5]. Structurally, MaSp are composed of three main parts—a nonrepetitive amino-terminal domain (NTD), a nonrepetitive carboxyl-terminal domain (CTD), and a highly repetitive core domain [6].

2 | Recombinant Spider Silk Production

To provide sufficient amounts of spider silk for applications, alternative production methods are required since most spiders are cannibals, making farming impractical [7]. Thus, two critical steps are necessary to produce biomimetic silk fibers without spiders: recombinant production of nature-like spidroins as well as a suitable spinning process [8].

To produce recombinant spidroins, genetic engineering of the underlying genes is established in several research groups. To replicate the properties of the natural silk, the genetic information has to be analyzed first (Figure 2). Depending on the utilized approach, the designed constructs of the repetitive units differ in amino acid composition, number of repetitions, and molecular weight [9].

Additionally, different host systems like insect cells, mammalian cells, yeast, transgenic animals, or bacteria have been reported over the years [10–14]. Every host comes with challenges and advantages, which further changes the outcome of the recombinant production. In this work, the recombinant production of intermediate molecular weight spidroins in microbial organisms is briefly described.

First, spidroin-encoding genes have to be extracted from the spider. Due to the highly repetitive sequences and a different codon usage than in most microbial hosts, the genes have to be modified for recombinant production. Most critical are the repetitive amino acid motifs within the core domain of the gene, mainly important for the silk's mechanical properties. In order to enable the efficient recombinant production of such highly repetitive sequences, consensus sequences have to be identified, then multimerized, and finally incorporated into a plasmid. As hosts, genetically engineered yeast or bacteria have been used and fermented under controlled conditions. Upon spidroin production, they are extracted and purified through a series of downstream processing steps, resulting in nonfibrous spidroins, which could, e.g., be freeze-dried for storage. Such spidroins serve as the foundation for fiber production [14].

Unlike natural spider silk proteins (250–350 kDa), the repetitive core domain of the recombinant spider silk ones is often smaller, depending on the protein variant used. Limitations in, e.g., bacterial expression hosts lead to decreasing yields with increasing molecular weight of the desired proteins [9]. In part, the yield of high molecular weight recombinant spidroins (up to 256 kDa) can be increased by lowering the induction temperature [15]. However, this approach is not feasible for every recombinant silk protein and every host organism.

Further, natural spider silk proteins are stored in the dope at concentrations up to 50% w/v, without triggering assembly processes. In contrast, for recombinantly produced spider silk, the limit is in the range of 20%–30% w/v [16]. One exception is mini spidroins, as shown by Schmuck et al., which had a high solubility of up to 50% w/v in aqueous buffers.

In nature, the main functions of the NTDs and CTDs are to provide solubility of the spidroins in the aqueous dope and also the initiation of fiber assembly in the duct upon external

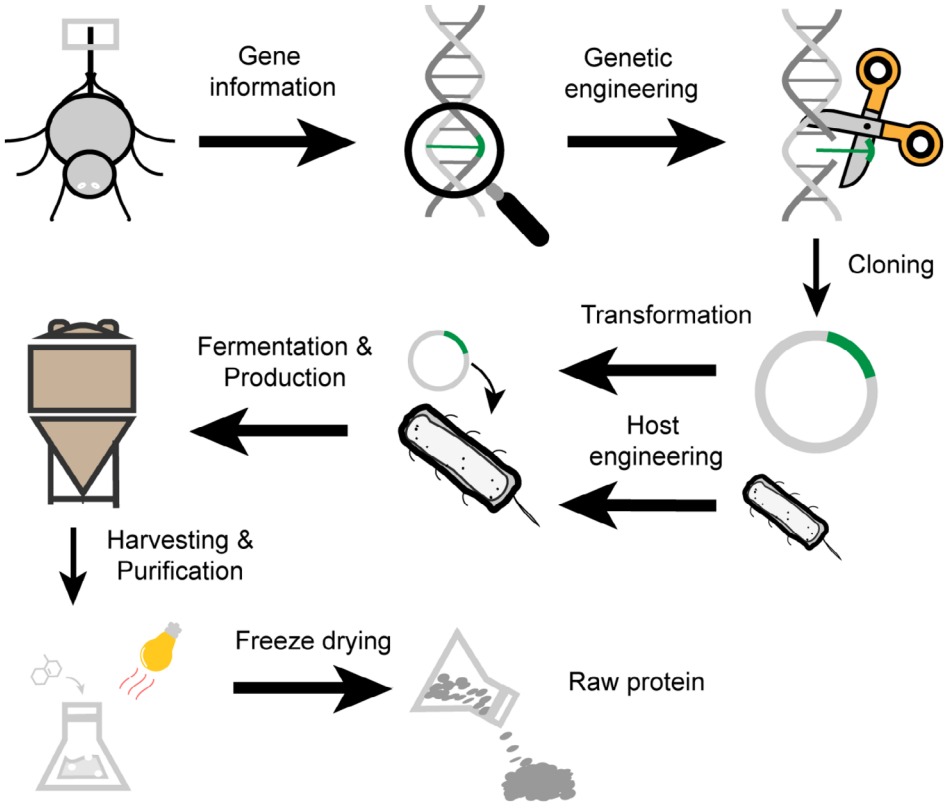

FIGURE 2 | Exemplary process of recombinant production of spider silk proteins. Genetic information regarding the spider silk proteins is extracted from the spider. The genes are modified and then transformed with a plasmid into an engineered host, typically of bacterial or yeast origin. The host is fermented and produces the protein of interest. The host cells are harvested, and the proteins are purified in several steps until the protein is obtained with the wanted purity, and then it can, e.g., be freeze-dried for storage.

triggers [17]. For recombinant spidroins, the NTDs and CTDs have the same function, but this is only true for aqueous dopes [18]. For nonaqueous solvents, the terminal domains are neither needed to dissolve the recombinant spidroins nor for fiber formation [19].

3 | Natural Spider Silk Assembly

Spider silk fiber assembly begins with the secretion of spidroins into the tail of a spider's silk gland (Figure 3A) [22]. In the gland, spidroins assemble within the ampulla into micelle-like structures for storage upon liquid–liquid phase separation (LLPS) [23–25]. In the spinning duct, shear stress, acidification, and salting-out mechanisms trigger further spidroin self-assembly [26, 27]. This process involves structural rearrangements of the NTDs and the CTDs, which are crucial for silk assemblies by forming a continuous spidroin network [18]. Acidification triggers a pH drop, promoting end-to-end multimerization of spidroin chains via the NTD and partially unfolding the CTD [28]. Shear forces generated by pultrusion of the dope in the duct align the preassembled spidroins, forming β-sheet nanocrystals [29]. The preformed fibers then start to solidify upon water resorption by the surrounding tissue and shear stress caused by the narrowing duct diameter and upon active drawing from the spider's abdomen [30]. The hierarchical molecular organization of the spidroins achieves an exceptional balance of elasticity and strength in the final fiber (Figure 3B) [31].

4 | Wet Spinning of Spidroins

Spinning dopes comprising recombinantly produced spidroins have to be prepared in specific ways prior to spinning. Often, denaturing agents like guanidium salts or urea are used to first dissolve the protein, followed by dialysis into buffered aqueous solutions. To achieve an aqueous spinning dope at necessary high concentrations, a dialysis against PEG can be utilized. Nonaqueous solvents for recombinant spider silk proteins include hexafluoroisopropanol (HFIP) or formic acid. The chosen solvent influences the dope's viscosity and also the fiber formation process. Thereby, not only the fiber diameter but also the resulting secondary structures of the underlying proteins are influenced. For instance, fibers produced via classical electrospinning have the lowest diameter when spun using a spinning dope with formic acid as solvent, intermediate diameters are achieved using HFIP as solvent, and the highest ones when using aqueous solutions [32]. Further, fibers spun from aqueous solutions show a higher amount of β-turns and random coil structures compared to those spun out of HFIP, where the relative amount of α-helix is higher. Both show the same amount of β-sheets after spinning [33, 34].

Posttreatment of artificially spun spider silk fibers aims to increase the mechanical performance and to induce water insolubility. The relative amount of β-sheets in the secondary structure directly influences the water solubility as well as the tensile strength of the fibers. To increase β-sheet content, heat treatment or alcohol treatment can be used, and among alcohols,

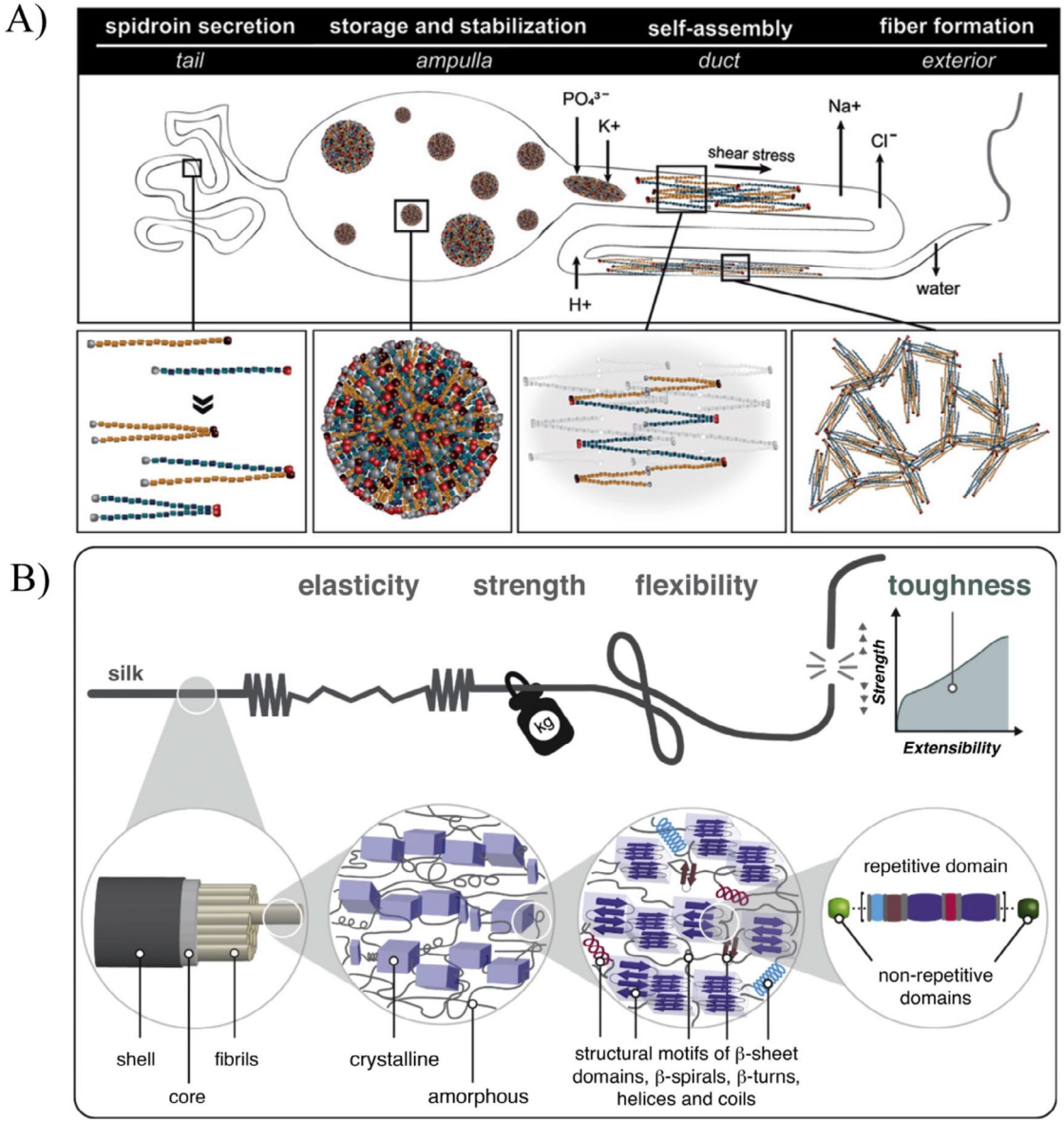

FIGURE 3 | Sketch of the putative spider silk assembly process in vivo and how it is mimicked using in vitro approaches. (A) Spidroin secretion in the tail. The different dimeric spidroins in the ampulla are packed in micellar-like assemblies upon liquid–liquid phase separation at a high concentration. Shear stress, ion exchange, and acidification lead to self-assembly of the spidroins into fibers, which are finally drawn from the spinning duct. Reproduced with permission from [20]. 2021, John Wiley and Sons. (B) An illustration depicting the hierarchical structure of spider silk, showcasing its exceptional toughness. Each silk fiber is made of fibrils with nanometer-sized crystallites within an amorphous matrix. The nanocrystals consist of well-ordered β-sheets, while the matrix includes β-spirals, β-turns, random coils, and helices. The silk's mechanical properties, like elasticity and strength, depend on the distribution and quantity of these structural motifs. Stress–strain analysis reveals toughness as the integral of the curve. Adapted with permission from [21]. 2019, Elsevier.

methanol induces beta sheet formation faster than, e.g., isopropanol [35].

Among the various methods for artificial spider silk fiber production, wet spinning stands out as a simple and cost-efficient technique for producing continuous fibers [36]. A noteworthy example of wet-spun silk mimetic fibers is the biotech spider silk fiber Biosteel, developed by AMSilk GmbH. This material displays properties comparable to that of natural spider silk and has demonstrated potential for commercialization [37]. In principle, wet spinning involves the extrusion of a spinning dope through a needle into a coagulation bath, where the dope solidifies into fibers. These fibers are subsequently collected on a winding unit outside the coagulation bath and dried thereafter. Despite its simplicity and low cost, the system's functionality can be enhanced by incorporating additional technical features to improve fiber properties. For example, Copeland et al. introduced multiple godets and two stretch baths before the winding unit to improve mechanical properties through poststretching (Figure 4A) [38].

During poststretching, the alignment of crystalline domains and the compaction of the overall structure led to an increased degree of crystallinity in the material [39]. While this posttreatment

approach significantly enhanced the fiber's strength and extensibility compared to as-spun fibers (Figure 4B), the mechanical performance of natural spider silk still remained unmatched at that time.

5 | Biomimetic Spinning

Different groups have attempted to produce fibers reaching the mechanical performance of natural silk by as close as possible replicating the natural spinning process. The results showed that the closer the natural process is mimicked, the better the mechanical properties of the fibers are. An example was shown by Peng et al. [40]; In addition to wet spinning, a microchip was implemented before the coagulation bath to simulate the narrowing duct diameter and inducing shear stress. The resulting fibers exhibited a maximum stress of approximately 500 MPa before rupture, more than twice the strength of the previously reported wet-spun fibers. Unfortunately, the mechanical properties showed great deviations.

In general, microfluidic-based systems hold significant promise for mimicking the key steps of the intricate processes occurring within spiders [41]. Within microchip channels controlled mixing of reactants is possible, providing fine-tuned regulation of chemical and physical reactions akin to the natural process [42]. For instance, in the work of Chen et al., the fiber spinning process is mimicked through two sequential intersections of a microchip: the first induces LLPS, followed by the second intersection, where nanofibrillation occurs due to a pH and salt gradient.

External air pultrusion assimilates the fiber's natural drawing, culminating in the formation of biomimetic fibers (Figure 5A) [43]. The resulting fibers consist of bundled fibrils, closely resembling the hierarchical architecture observed in natural spider silk (Figure 5B).

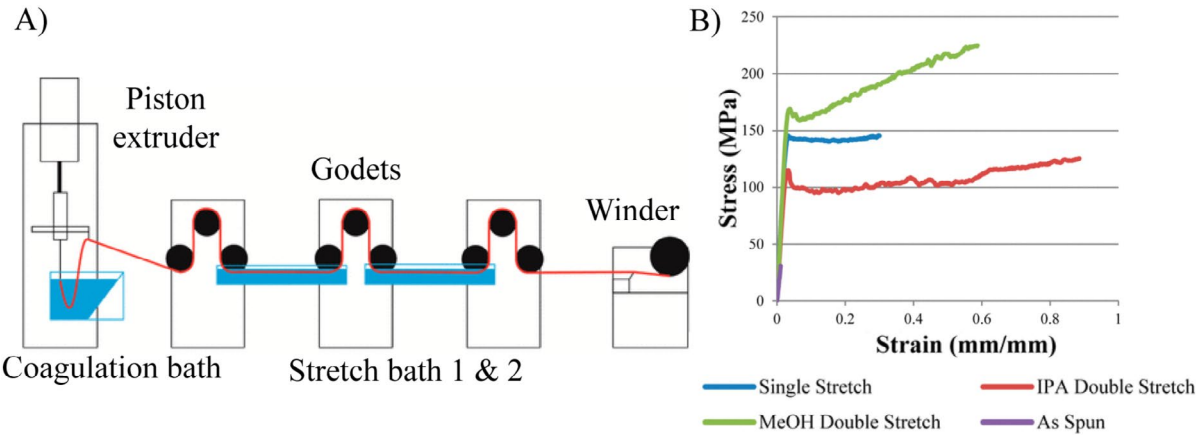

FIGURE 4 | Wet spinning of spider silk proteins. (A) Schematic setup of a wet-spinning device with two poststretch baths to increase the mechanical properties of the recombinant spider silk. (B) Mechanical evaluation of wet-spun recombinant silk fibers as-spun, single, and double stretched in methanol (MeOH) or isopropanol (IPA). Adapted with permission from [38]. Copyright 2015, American Chemical Society.

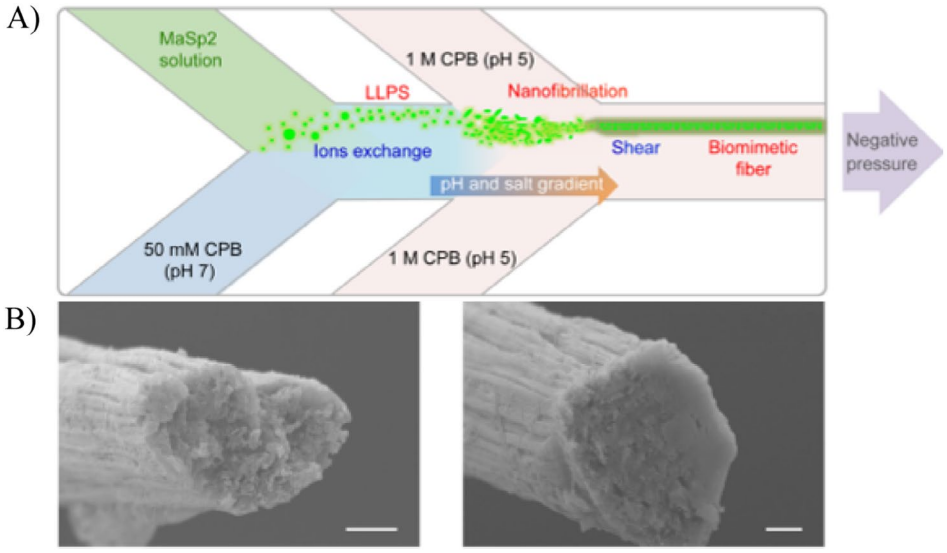

FIGURE 5 | Microfluidic-chip approach for biomimetic spinning. (A) Scheme of the channels of a microfluidic chip used for biomimetic spinning. Reproduced under the terms of the Attribution 4.0 International (CC-BY 4.0) license [43]. Copyright 2024, Springer Nature. (B) The hierarchical fibril structure of two different biomimetically spun fibers (scale bars 5 μm), which is similar to the natural one (not shown). Adapted under the terms of the Attribution 4.0 International (CC-BY 4.0) license [43]. Copyright 2024, Springer Nature.

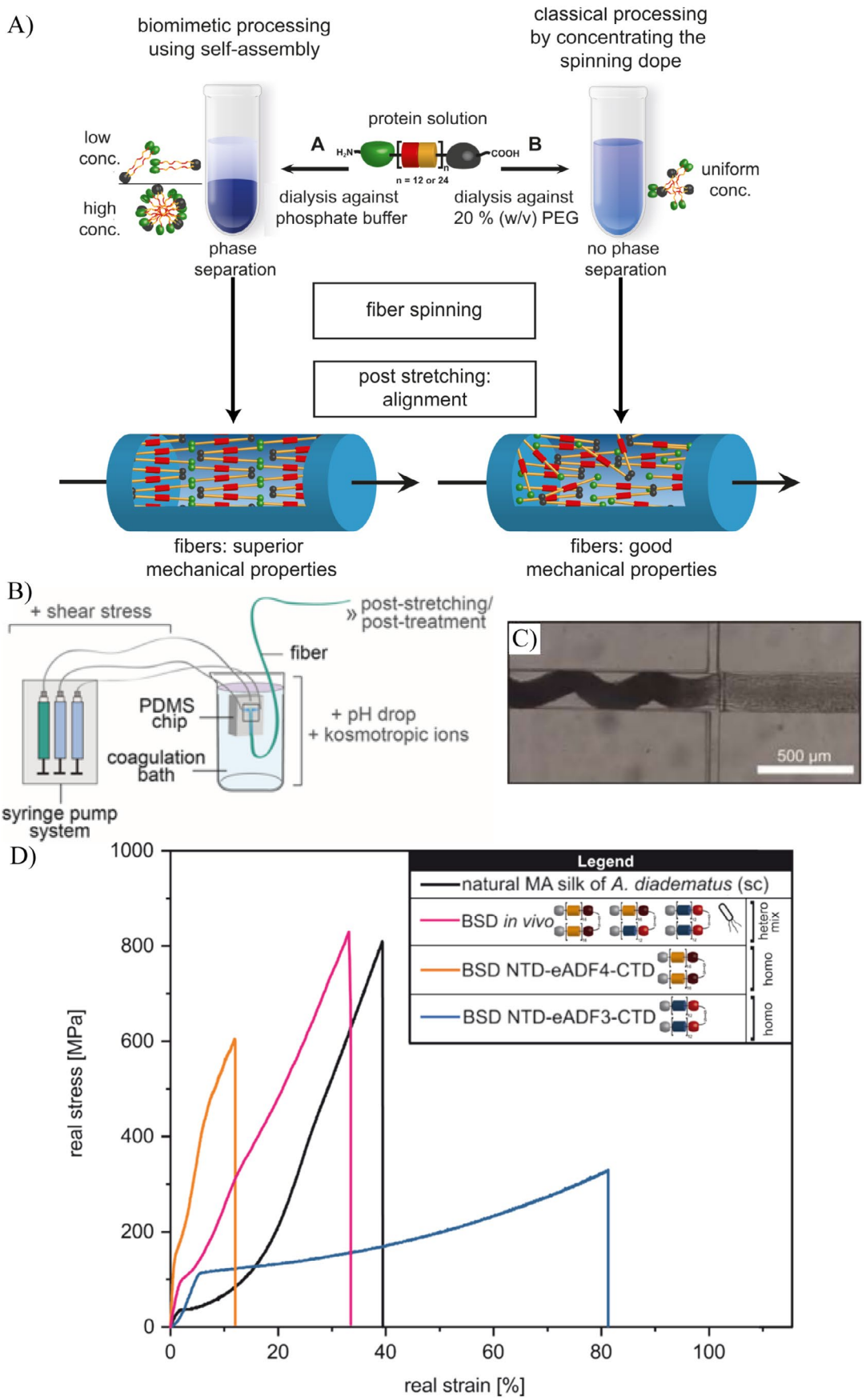

FIGURE 6 | Legend on next page.

FIGURE 6 | Biomimetic spider silk spinning. (A) Comparison of dope processing methods regarding the mechanical properties of the resulting fibers, with biomimetic spinning dopes (BSD) promoting phase separation versus classical spinning dopes (CSD) without phase separation. Adapted with permission from [44]. 2015, John Wiley and Sons. (B) Biomimetic spinning of BSD and CSD using a microfluidic device including phosphate buffers as sheath solution and a phosphate-containing coagulation bath to obtain mechanically strong fibers. Reproduced with permission from [45]. 2023, American Chemical Society. (C) Zoom-in of the microchip inlet of (B) inducing fiber formation. Reproduced with permission from [20]. 2021, John Wiley and Sons. (D) Mechanical evaluation of homodimers of eADF4 and eADF3, a heterodimer/homodimer mix of eADF4/eADF3, and natural MA silk fibers of *Araneus diadematus*.

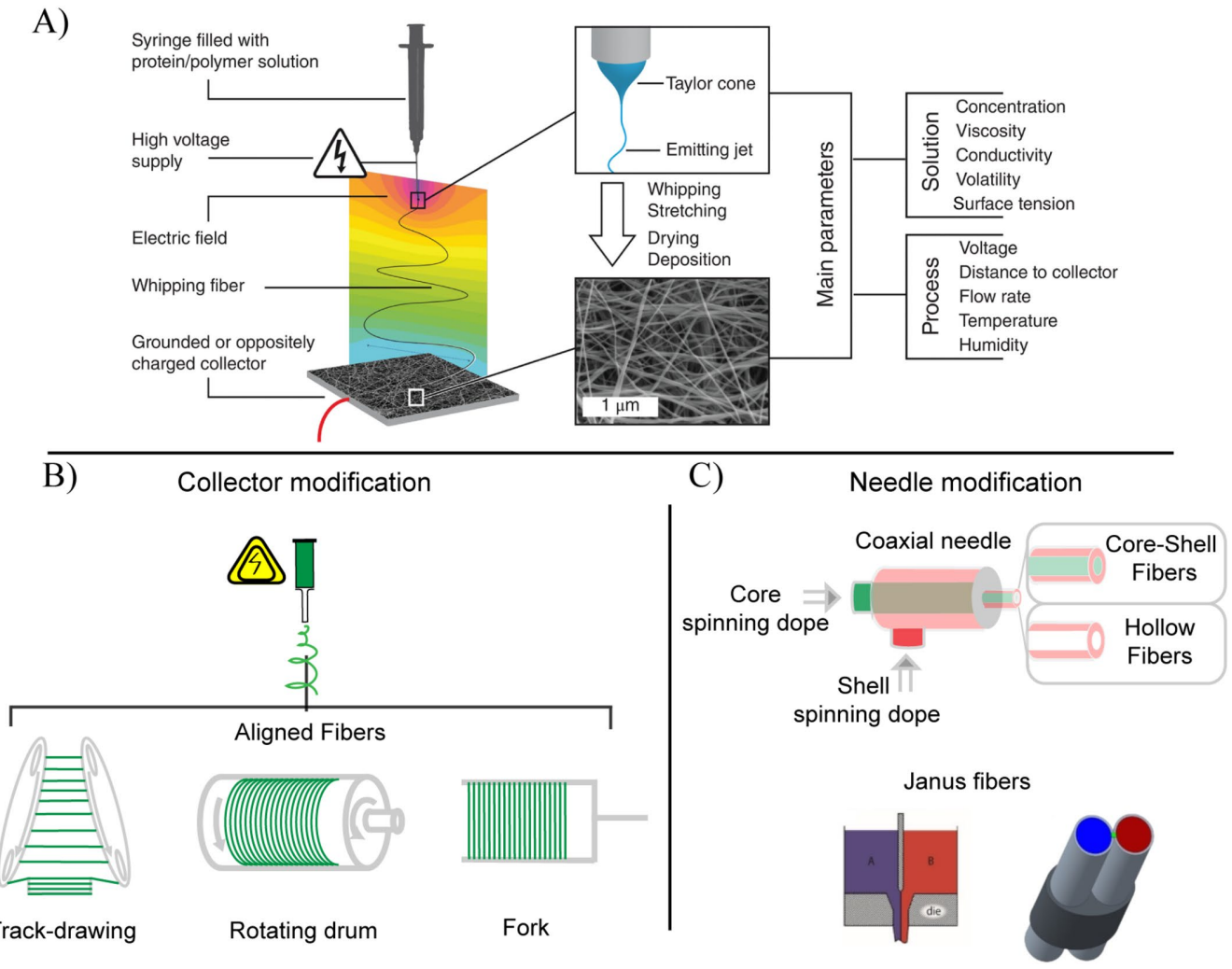

FIGURE 7 | Electrospinning set-ups. (A) Illustration of a usual electrospinning setup and corresponding parameters. Reproduced with permission from [48]. Copyright 2018, John Wiley and Sons. (B) The collector modifications transform the fibers from a random to an aligned orientation. With a track-drawing device, defined poststretching of the fibers can be obtained. The fibers collected using a rotating drum are aligned along the rotational axis. The fork collector offers an opportunity to transfer aligned fibers easily. (C) By changing needle geometry, different fiber morphologies, like core-shell, hollow, or Janus fibers, can be created, opening the road toward novel applications. As an example, the efficiency of catalytic reactions can be improved at the interface of two different fibers spun together (Janus fiber) [49]. Adapted under the terms of the Attribution-NonCommercial 4.0 International (CC BY-NC 4.0) license [50]. Copyright 2023, John Wiley and Sons.

In another approach, the process started with an alternative preparation of the spinning dope. Heidebrecht et al. implemented a new technique for preparing biomimetic spinning dopes (BSD) and compared them with classical spinning dopes (CSD) (Figure 6A) [44]. In BSD, LLPS was induced, resulting in a high-density protein-rich micellar phase and a low-density phase, whereas CSD only showed a single phase. Spinning of the high-density phase of BSD resulted in better mechanical properties of the spun fibers. Subsequently, Saric et al. [20] adopted the process of spinning dope preparation and added another facet to the process: Spider silks are typically made of more than one type of spidroin, and based thereon, instead of one, two different recombinant spider silk proteins, namely eADF3 and eADF4, were employed. Spinning of such two-protein BSDs using a microfluidic chip simulated several conditions found in the natural process occurring in a spider's spinning duct (Figure 6B,C). The fiber assembly was finalized using poststretching and post-treatment, yielding fibers with mechanical properties closely

resembling that of natural spider silk (Figure 6D). In comparison, fibers formed from either eADF3 or eADF4 alone displayed inferior mechanical performance, highlighting the advantage of the double-spidroin approach.

6 | Electrospinning of Spidroins

The processing of recombinant silk proteins into fibers is not only limited to nature-like techniques but extends to fully artificial production of submicron- and nanofibers. The surface-to-volume ratio increases significantly in this dimension, changing the fibers' properties. Such fibers can be, e.g., produced using electrospinning upon extruding the spinning dope through a needle into an electrical field. Charges accumulate on the molecular chains inside the dope until their repulsion exceeds the surface tension [46]. A Taylor cone forms, from which a prefiber is ejected. Instabilities along the fiber caused by uneven solvent evaporation are launching whipping, which induces fiber stretching [47]. Subsequently, the fiber's diameter decreases, and the fibers are deposited randomly on a flat collector (Figure 7A) [51]. By replacing a flat collector with either a track-drawing

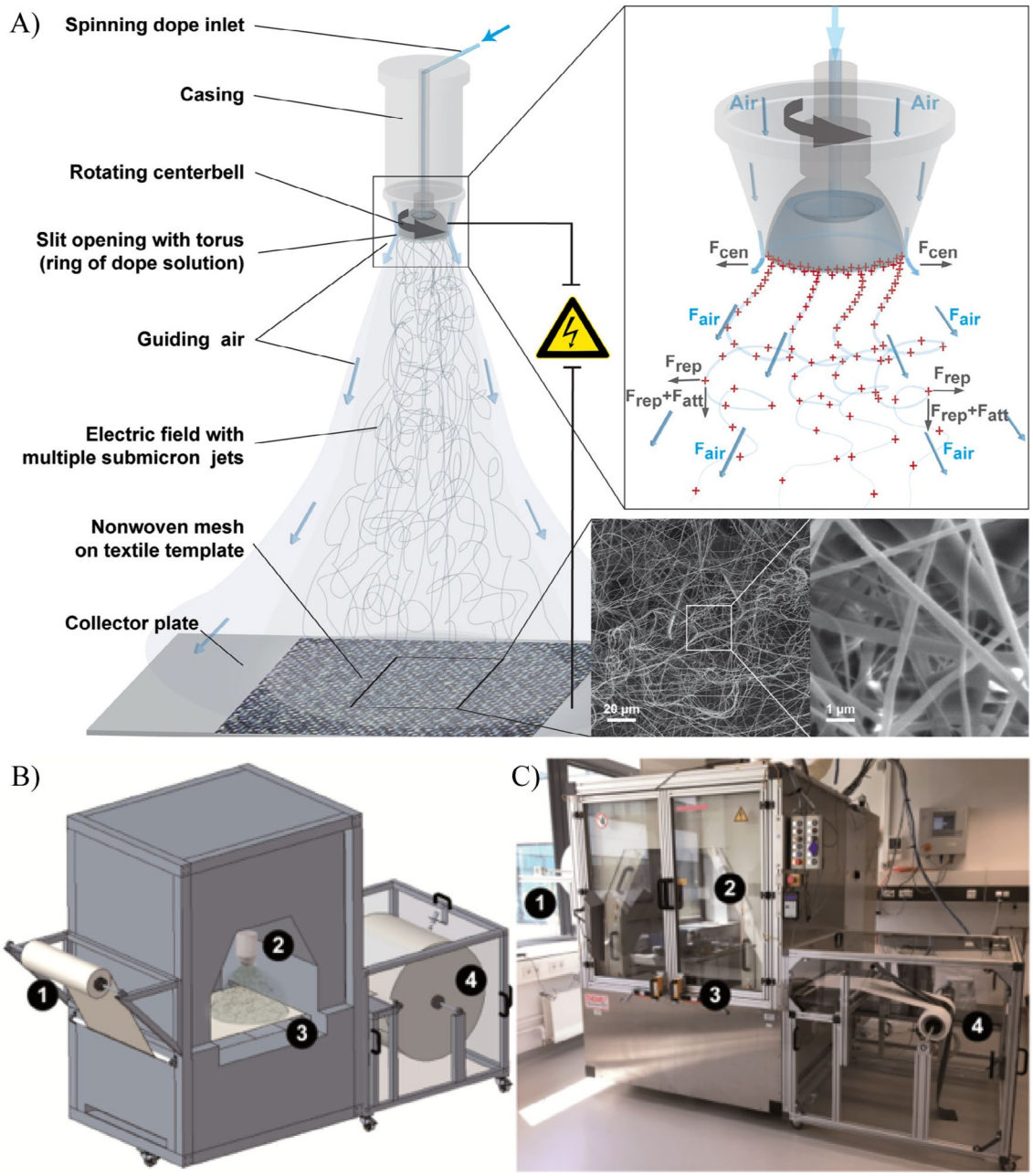

FIGURE 8 | Centrifugal electrospinning. (A) In order to increase the throughput of an electrospinning setup, the often used needle can be replaced by a rotating center bell. Centrifugal forces and electrical repulsion lead to fiber formation at high speeds and allow for up-scaling. Reproduced with permission from [57]. Copyright 2020, American Chemical Society. Scheme (B) and photograph (C) of continuous spider silk centrifugal electrospinning in a roll-to-roll process. A substrate (1) is unwound and transferred into the spinning chamber, where the centrifuge (2) ejects fibers onto the collector (3) coating the substrate. Subsequently, the substrate is collected on a winder (4). Reproduced under the terms of the Attribution 4.0 International (CC-BY 4.0) license [33]. Copyright 2020, MDPI.

device, a rotational drum, or a two-stick fork, aligned single fibers can be manufactured (Figure 7B) [52]. In the case of a track-drawing device, the fibers are emitted between two conveyors in parallel and transported onto a collector in a perpendicular fashion. Adjusting the conveyors' spacing enables controlled poststretching of the fibers [53]. Rotational drums achieve alignment through high-speed rotation, directing fibers along the axis of rotation [54]. Additionally, fibers can be removed locally or as a whole from the drum to create tubular structures, further expanding their potential applications [32]. The simplest method for aligned fibers uses a fork, where the fibers orient between the two sticks.

Alterations in the needle design in an electrospinning set-up can yield additional fiber features. In this approach, the standard needle is replaced with coaxial or Janus needles (Figure 7C). Coaxial needles consist of one needle concentrically embedded within another one, enabling the production of core-shell fibers from two distinct materials [55]. By utilizing a sacrificial core material, this technique can also generate hollow fibers [56]. Janus fibers are produced by modifying the needle geometry to position the spinning dopes side-by-side. This configuration enables the creation of unique interfacial geometries between two distinct materials, which is especially important for catalytic reactions, where the spatial proximity is directly related to the catalytic efficiency [49, 50]. Despite the versatility and potential of electrospinning, its low material throughput renders it, in most cases, less useful for industrial-scale applications.

7 | Centrifugal Electrospinning

A promising approach for scaling up the production of submicron- or nanofibers via electrospinning is its combination with centrifugal spinning. With a throughput of up to 1000 times higher than in conventional needle-based electrospinning, this technology holds significant promise, exemplarily in the production of filter membranes. A rotating center bell replaces a simple nozzle in this method. The spinning dope is propelled outward by centrifugal forces and ejected at the edge of the bell, where multiple Taylor cones form simultaneously. The fibers are further accelerated and directed by an electric field and guiding airflow, ensuring precise deposition and alignment of the fibers (Figure 8A) [57]. A schematic (Figure 8B) and a photograph (Figure 8C) illustrate the device and its components. Designed for filter membranes, the system accommodates 2D substrates (1), which are fed into the spinning chamber. Within the chamber, the spinneret (2) deposits fibers onto any substrate on a collector (3), and the coated substrate is then collected on the winder (4), finally yielding a roll-to-roll process.

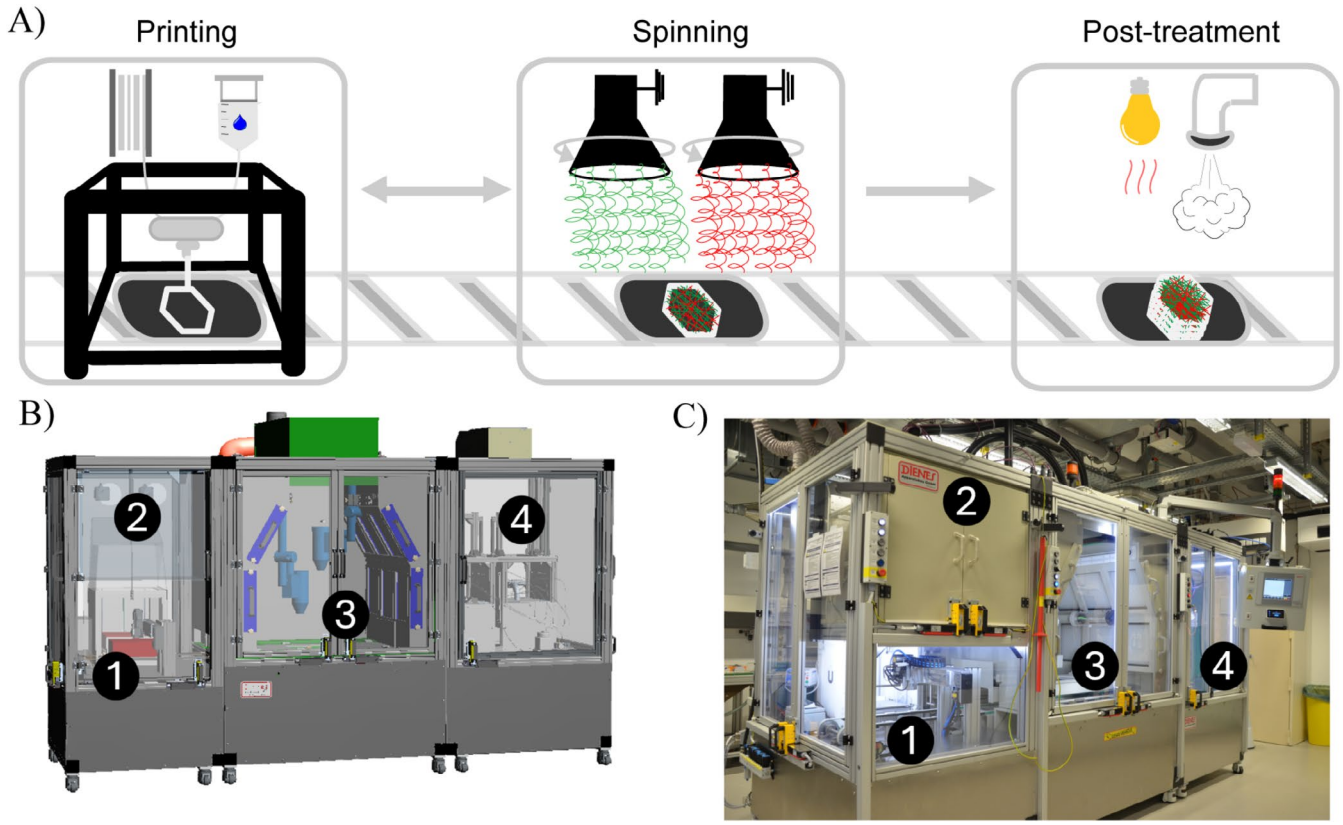

FIGURE 9 | Combined 3D-printing and centrifugal electrospinning. (A) Scheme of a 3-in-1 device to fabricate hierarchical structures using 3D-printing, a two-head centrifugal electrospinning device, and an integrated posttreatment chamber. The sample can be transferred from printing to spinning to create hierarchical structures in a fully automated process. The printer is fed with either filaments or hydrogels. The spinning device has two independently working center bells, which can be loaded with different spinning solutions. The posttreatment chamber allows changing the structural properties, especially of protein-based fibers. CAD model (B) and photograph (C) of the 3D-centrifugal spinning device with a 3D-printer (1), spinning dope chamber (2), spinning chamber (3), and posttreatment chamber (4).

In order to achieve hierarchical structures spanning from the nano- to the macroscale, centrifugal electrospinning can be combined with 3D-printing. The workflow is illustrated in Figure 9A, while a 3D design is provided in Figure 9B and a photograph is shown in Figure 9C. The 3-in-1 device incorporates a 3D printer (1) capable of fused deposition molding or dispense plotting. Spinning dopes can be loaded into the spinning dope chamber (2). The centrifugal electrospinning chamber holds two individually operating center bells (3), enabling the spinning of two types of fibers simultaneously. A conveyor belt transfers the samples between the printing and spinning chambers, which can be repeated several times in order to achieve the desired structural complexity. Finally, the construct is moved to the posttreatment chamber (4), where its properties can be enhanced through chemical or heat treatments.

The major advantage of this device is the use of two different processing technologies in one set-up yielding completely different morphologies of spider silk. In the 3D printing device, a spider silk hydrogel can be dispense-plotted to build a scaffold with several hundred-micrometer wide struts. Layers of spider silk nanofibers can be deposited thereon using a centrifugal electrospinning module. The two morphologies can be alternated until the desired overall 3D structure is achieved.

8 | Yarn Electrospinning

Another possibility to fabricate hierarchical structures along different length scales is yarn electrospinning. Upon modification of the basic electrospinning setup, a bundle of nanofibers can be processed into a thread. The fibers are assembled along the yarn axis, coherently enhancing the resilience against rupture when handled [58]. These yarns can be further assembled into superstructures through techniques such as weaving, braiding, or knitting, allowing the fabrication of complex geometries [59].

To yield yarns in an electrospinning set-up, oppositely charged spinnerets are positioned facing each other with a rotating fiber collector placed in between (Figure 10A). The oppositely charged

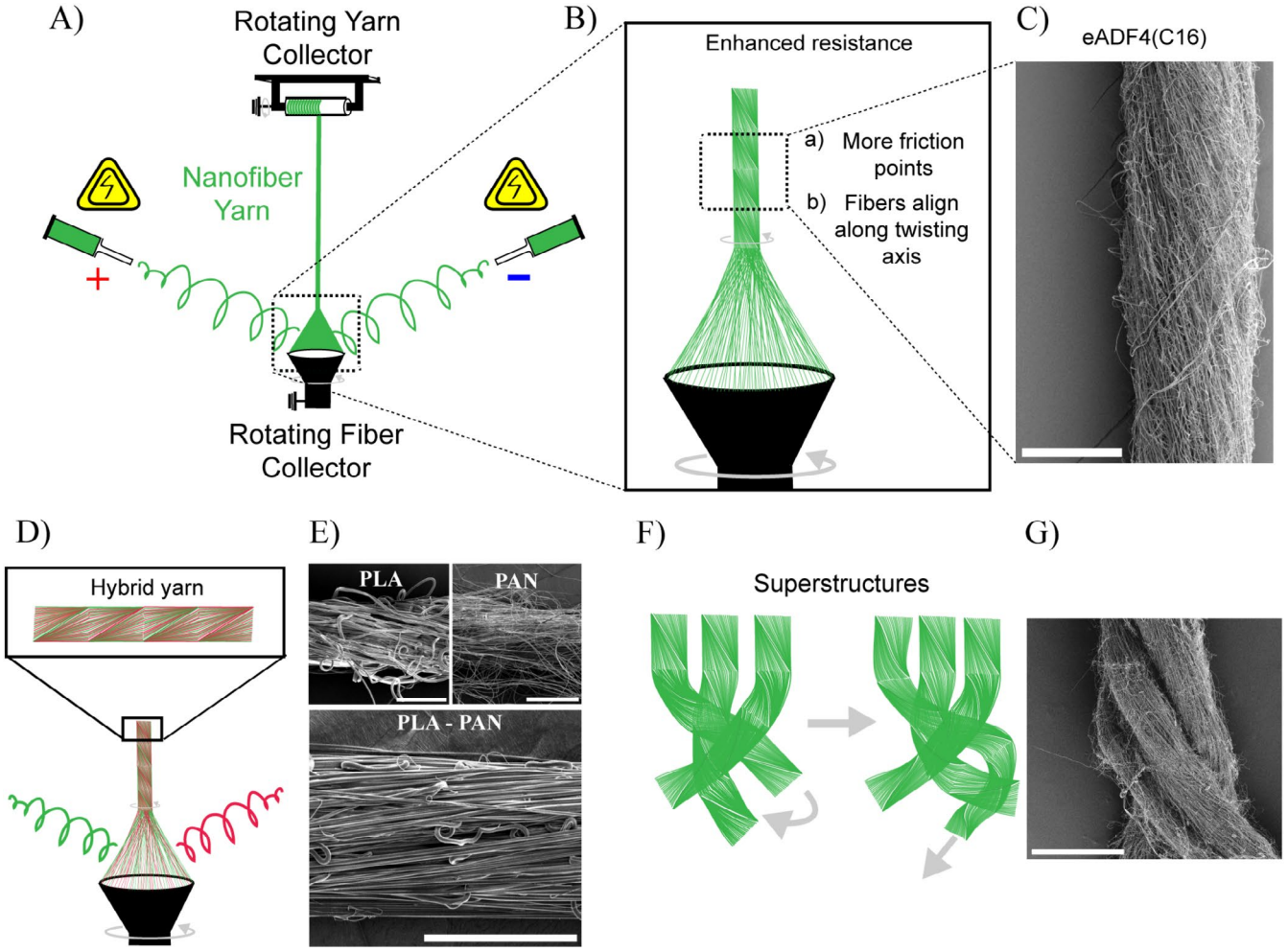

FIGURE 10 | Yarn electrospinning. (A) Schematic setup of yarn electrospinning. The adjusted spinnerets eject oppositely charged fibers on a rotating collector yielding a cylindrical fiber mesh. At the top of the fiber cone, a yarn is forming and ultimately winded onto the rotating yarn collector. (B) The advantages of nanofiber yarns over conventional meshes are (a) more friction points between the fibers and (b) a fiber direction along the twisting axis resulting in improved resistance toward external force. (C) SEM image of an eADF4(C16) + 1% PEO (400 kDa) nanofiber yarn (scale bar 100 μm). (D) Two spinnerets allow the use of two different spinning dopes to manufacture composite yarns. (E) SEM images of individual PLA and PAN nanofiber yarns and a composite PLA-PAN nanofiber yarn (scale bar 50 μm). (F) Nanofiber yarns can be braided into superstructures. (G) SEM image of entangled multifilament nanofiber yarn made of PAN (scale bar 500 μm).

TABLE 1 | Spinning techniques to create different fiber morphologies using recombinant spider silk proteins.

Wet spinning			
Silk fibroin	MaSp1:MaSp2 (1:4)	MaSp1	MaSp2
Solvent concentration	HFIP:FA (4:1), 25% w/v	HFIP, 20% w/v	HFIP, 45%–60% w/v
Molecular weight	65 kDa	284 kDa	86.5 kDa
Host	Transgenic goat	Bacterial	Bacterial
Spider species	*Nephila clavipes*	*N. clavipes*	*N. clavipes*
Mechanical properties	Tensile strength: 221.72 ± 11.01 MPa	Tenacity: 508 ± 108 MPa	Tensile strength: 53.5 ± 18.0 MPa
Geometrical complexity	Monofilament	Monofilament	Monofilament
Troughput	0.7 mm/min	1–2 mL/h	0.5 mm/min
Utility	Protein-based fiber material	Protein-based fiber material	Protein-based fiber material
Reference	[38]	[19]	[60]
Biomimetic spinning			
Silk fibroin	eADF3/eADF4 (1:1)	NT2RepCT	eADF3
Solvent concentration	Aqueous, 15% w/v	Aqueous, 30% w/v	Aqueous, 10%–15% w/v
Molecular weight	76/74 kDa	33 kDa	76 kDa
Host	Bacterial host	Bacterial host	Bacterial host
Spider species	*A. diadematus*	*Euprosthenops australis*, *Araneus ventricosus*	*A. diadematus*
Mechanical properties	Tensile strength: 834 ± 34 MPa	Tensile strength: 261 ± 77 MPa	Tensile strength: 383 ± 113 MPa
Geometrical complexity	Monofilament	Monofilament	Monofilament
Troughput	50–150 μL/h	17 μL/min	n.a.
Utility	Protein-based fiber material	Protein-based fiber material	Protein-based fiber material
Reference	[20]	[61]	[44]
Electrospinning			
Silk fibroin	eADF4	pNSR32	eADF4
Solvent concentration	HFIP, 10% w/v	Formic acid, 5% protein content/95% PCL	HFIP, 5%–25% w/v
Molecular weight	48 kDa	102 kDa	48 kDa
Host	Bacterial	Prokaryotic	Bacterial
Spider species	*A. diadematus*	n.a.	*A. diadematus*
Mechanical properties	Tensile strength: 81.1 ± 8.9 MPa	Not measured	Not measured
Geometrical complexity	Fiber mat; twisted by hand for mechanical evaluation	Tubular nonwoven	Coating for filter applications
Troughput	14 μL/min	80 μL/min	4.4 μL/min
Utility	Filter system	Vascular graft	Filter coating
Reference	[35]	[61]	[62]

(Continues)

TABLE 1 | (Continued)

Spinning technique	Centrifugal electrospinning	Yarn electrospinning
Silk fibroin	eADF4	eADF4
Solvent concentration	HFIP, 1%–8% w/v	n.a.
Molecular weight	48 kDa	48 kDa
Host	Bacterial host	Bacterial host
Spider species	*A. diadematus*	*A. diadematus*
Mechanical properties	Not measured	1.57 ± 0.57 MPa
Geometrical complexity	Fiber mat	Nanofiber yarn
Troughput	1–8 mL/min	18 cm/min
Utility	Filter coating	Biomaterial
Reference	[33]	[63]

fibers neutralize their charges as they assemble into a cylindrical fiber mesh on the collector. As the fiber collector rotates, the cylindrical fiber mesh twists into a yarn, which is subsequently collected by a winding unit. Figure 10B highlights the enhanced resistance of yarns compared to single fiber bundles, emphasizing the alignment of fibers along the yarn axis, which increases the number of fiber-to-fiber friction points, leading to improved manageability. A yarn spun from the recombinant spider silk protein eADF4(C16) is shown in Figure 10C, where the fibers are oriented diagonally along the twisting axis. Using two spinnerets also enables the simultaneous spinning of different materials to produce hybrid yarns, as demonstrated in Figure 10D. In this example, elastic polylactic acid (PLA) and rigid polyacrylonitrile (PAN) were spun individually or combined to form a composite material (Figure 10E). The SEM image of the individual PLA yarn reveals fiber loops, which are also visible in the hybrid yarn. In contrast, the PAN yarn exhibits straighter fibers, resulting in an alternating fiber arrangement within the hybrid yarn. Figure 10F illustrates a method for creating superstructures by braiding multiple yarns, showcasing the potential for advanced material fabrication.

9 | Conclusions and Outlook

The outstanding mechanical properties of spider silk have inspired researchers to unravel the underlying principles and further mimic them in man-made processes. Harvesting spider silk from spiders is inefficient due to their cannibalistic behavior. Therefore, recombinant production techniques have been developed to produce the underlying spidroins, laying the foundation for further research. However, early attempts to generate fibers with nature-like properties using wet spinning resulted in fibers of inferior mechanical properties. This led to efforts mimicking as close as possible the natural spinning process.

Biomimetic spinning techniques significantly improved the mechanical performance of recombinant spider silk fibers. New concepts such as microfluidic-assisted spinning, double-spidroin designs, and optimized dope preparation resulted in enhanced strength, toughness, and consistency of these fibers.

Nonnatural spinning methods like electrospinning enable the production of submicron- to nanometer-scale fibers, leading to new fields of applications such as in filter membranes. Modifications of the electrospinning setup have expanded the versatility of these fibers, including the ability to produce aligned meshes or specific interfaces. Centrifugal electrospinning has further advanced the range of applications by increasing the throughput by a factor of 1000, making large-scale applications feasible. A summary of the different spinning techniques to create fibers using recombinant spider silk is given in Table 1. For an extended list of wet spinning and biomimetic spinning, we refer to the review article of Koeppel and Holland [64].

As a future perspective, the combination of 3D printing with centrifugal electrospinning will enable the creation of complex hierarchical structures, while yarn electrospinning facilitates the fabrication of threads that can be processed into superstructures, opening new possibilities in areas like tissue engineering.

Acknowledgments

The authors acknowledge the support of the TAO Keylab Fiber spinning. The manuscript has been proofread by Dr. Hendrik Bargel and M.Sc. Thomas Ebbinghaus.

Conflicts of Interest

The authors declare the following competing financial interest(s): Thomas Scheibel is the founder and shareholder of AMSilk GmbH. Manuel Michel declares no conflicts of interest.

References

1. Y. Liu, Z. Shao, and F. Vollrath, "Relationships Between Supercontraction and Mechanical Properties of Spider Silk," *Nature Materials* 4 (2005): 901–905.

2. F. K. Ko and J. Jovicic, "Modeling of Mechanical Properties and Structural Design of Spider Web," *Biomacromolecules* 5 (2004): 780–785.

3. E. Doblhofer, A. Heidebrecht, and T. Scheibel, "To Spin or Not to Spin: Spider Silk Fibers and More," *Applied Microbiology and Biotechnology* 99 (2015): 9361–9380.

4. V. Fritz, "Strength and Structure of Spiders' Silks," *Reviews in Molecular Biotechnology* 74 (2000): 67–83.

5. J. Dionne, T. Lefevre, and M. Auger, "Major Ampullate Spider Silk With Indistinguishable Spidroin Dope Conformations Leads to Different Fiber Molecular Structures," *International Journal of Molecular Sciences* 17 (2016): 1353.

6. M. Hedhammar, A. Rising, S. Grip, et al., "Structural Properties of Recombinant Nonrepetitive and Repetitive Parts of Major Ampullate Spidroin 1 From *Euprosthenops australis*: Implications for Fiber Formation," *Biochemistry* 47, no. 11 (2008): 3407–3417, https://doi.org/10.1021/bi702432y.

7. L. R. Fox, "Factors Influencing Cannibalism, a Mechanism of Population Limitation in the Predator Notonecta Hoffmanni," *Ecology* 56 (1975): 933–941.

8. F. Teule, A. R. Cooper, W. A. Furin, et al., "A Protocol for the Production of Recombinant Spider Silk-Like Proteins for Artificial Fiber Spinning," *Nature Protocols* 4 (2009): 341–355.

9. A. Rising, M. Widhe, J. Johansson, and M. Hedhammar, "Spider Silk Proteins: Recent Advances in Recombinant Production, Structure–Function Relationships and Biomedical Applications," *Cellular and Molecular Life Sciences* 68 (2011): 169–184.

10. S. Ittah, S. Cohen, S. Garty, D. Cohn, and U. Gat, "An Essential Role for the C-Terminal Domain of a Dragline Spider Silk Protein in Directing Fiber Formation," *Biomacromolecules* 7 (2006): 1790–1795.

11. A. Lazaris, S. Arcidiacono, Y. Huang, et al., "Spider Silk Fibers Spun From Soluble Recombinant Silk Produced in Mammalian Cells," *Science* 295, no. 5554 (2002): 472–476, https://doi.org/10.1126/science.1065780.

12. S. R. Fahnestock and L. A. Bedzyk, "Production of Synthetic Spider Dragline Silk Protein in Pichia Pastoris," *Applied Microbiology and Biotechnology* 47 (1997): 33–39.

13. H.-T. Xu, F. Bao-Liang, Y. Shu-Yang, et al., "Construct Synthetic Gene Encoding Artificial Spider Dragline Silk Protein and its Expression in Milk of Transgenic Mice," *Animal Biotechnology* 18 (2007): 1–12.

14. T. Scheibel, "Spider Silks: Recombinant Synthesis, Assembly, Spinning, and Engineering of Synthetic Proteins," *Microbial Cell Factories* 3 (2004): 14.

15. Y.-X. Yang, Z.-G. Qian, J.-J. Zhong, and X.-X. Xia, "Hyper-Production of Large Proteins of Spider Dragline Silk MaSp2 by *Escherichia coli* via Synthetic Biology Approach," *Process Biochemistry* 51 (2016): 484–490.

16. M. Heim, D. Keerl, and T. Scheibel, "Spider Silk: From Soluble Protein to Extraordinary Fiber," *Angewandte Chemie (International Ed. in English)* 48 (2009): 3584–3596.

17. J. Bauer, D. Schaal, L. Eisoldt, K. Schweimer, S. Schwarzinger, and T. Scheibel, "Acidic Residues Control the Dimerization of the N-Terminal Domain of Black Widow Spiders' Major Ampullate Spidroin 1," *Scientific Reports* 6 (2016): 34442.

18. G. Askarieh, M. Hedhammar, K. Nordling, et al., "Self-Assembly of Spider Silk Proteins is Controlled by a pH-Sensitive Relay," *Nature* 465 (2010): 236–238.

19. X. X. Xia, Z. G. Qian, C. S. Ki, Y. H. Park, D. L. Kaplan, and S. Y. Lee, "Native-Sized Recombinant Spider Silk Protein Produced in Metabolically Engineered *Escherichia coli* Results in a Strong Fiber," *Proceedings of the National Academy of Sciences of the United States of America* 107 (2010): 14059–14063.

20. M. Saric, L. Eisoldt, V. Doring, and T. Scheibel, "Interplay of Different Major Ampullate Spidroins During Assembly and Implications for Fiber Mechanics," *Advanced Materials* 33 (2021): e2006499.

21. M. Saric and T. Scheibel, "Engineering of Silk Proteins for Materials Applications," *Current Opinion in Biotechnology* 60 (2019): 213–220.

22. J. R. Dos Santos-Pinto, A. M. Garcia, H. A. Arcuri, et al., "Silkomics: Insight Into the Silk Spinning Process of Spiders," *Journal of Proteome Research* 15, no. 4 (2016): 1179–1193, https://doi.org/10.1021/acs.jproteome.5b01056.

23. J. H. Exler, D. Hummerich, and T. Scheibel, "The Amphiphilic Properties of Spider Silks are Important for Spinning," *Angewandte Chemie International Edition* 46, no. 19 (2007): 3559–3562, https://doi.org/10.1002/anie.200604718.

24. F. Hagn, L. Eisoldt, J. G. Hardy, et al., "A Conserved Spider Silk Domain Acts as a Molecular Switch That Controls Fibre Assembly," *Nature* 465 (2010): 239–242.

25. A. D. Malay, T. Suzuki, T. Katashima, N. Kono, K. Arakawa, and K. Numata, "Spider Silk Self-Assembly via Modular Liquid-Liquid Phase Separation and Nanofibrillation," *Science Advances* 6, no. 45 (2020): eabb6030, https://doi.org/10.1126/sciadv.abb6030.

26. D. P. Knight and F. Vollrath, "Changes in Element Composition Along the Spinning Duct in a Nephila Spider," *Naturwissenschaften* 88, no. 4 (2001): 179–182, https://doi.org/10.1007/s001140100220.

27. A. Rising and J. Johansson, "Toward Spinning Artificial Spider Silk," *Nature Chemical Biology* 11 (2015): 309–315.

28. M. Andersson, G. Chen, M. Otikovs, et al., "Carbonic Anhydrase Generates CO_2 and H^+ That Drive Spider Silk Formation via Opposite Effects on the Terminal Domains," *PLoS Biology* 12, no. 8 (2014): e1001921, https://doi.org/10.1371/journal.pbio.1001921.

29. A. Koeppel, P. R. Laity, and C. Holland, "Extensional Flow Behaviour and Spinnability of Native Silk," *Soft Matter* 14 (2018): 8838–8845.

30. F. Vollrath and D. P. Knight, "Liquid Crystalline Spinning of Spider Silk," *Nature* 410 (2001): 541–548.

31. S. Keten, Z. Xu, B. Ihle, and M. J. Buehler, "Nanoconfinement Controls Stiffness, Strength and Mechanical Toughness of β-Sheet Crystals in Silk," *Nature Materials* 9 (2010): 359–367.

32. C. Sommer and T. Scheibel, "Suitable Electrospinning Approaches for Recombinant Spider Silk Proteins," *Open Ceramics* 15 (2023): 100420.

33. F. Müller, S. Zainuddin, and T. Scheibel, "Roll-to-Roll Production of Spider Silk Nanofiber Nonwoven Meshes Using Centrifugal Electrospinning for Filtration Applications," *Molecules* 25 (2020): 5540.

34. E. DeSimone, T. B. Aigner, M. Humenik, G. Lang, and T. Scheibel, "Aqueous Electrospinning of Recombinant Spider Silk Proteins," *Materials Science and Engineering C* 106 (2020): 110145, https://doi.org/10.1016/j.msec.2019.110145.

35. G. Lang, B. R. Neugirg, D. Kluge, A. Fery, and T. Scheibel, "Mechanical Testing of Engineered Spider Silk Filaments Provides Insights Into Molecular Features on a Mesoscale," *ACS Applied Materials & Interfaces* 9 (2017): 892–900.

36. J. Zhang, M. Gong, and Q. Meng, "Wet Spinning is Employed to Produce Spider Silk With High Elasticity," *APL Materials* 11, no. 8 (2023): 081110, https://doi.org/10.1063/5.0160351.

37. H. Bargel and T. Scheibel, "A Bio-Engineering Approach to Generate Bioinspired (Spider) Silk Protein-Based Materials," *at – Automatisierungstechnik* 72, no. 7 (2024): 657–665, https://doi.org/10.1515/auto-2024-0020.

38. C. G. Copeland, B. E. Bell, C. D. Christensen, and R. V. Lewis, "Development of a Process for the Spinning of Synthetic Spider Silk," *ACS Biomaterials Science & Engineering* 1 (2015): 577–584.

39. G. Greco, B. Schmuck, F. G. Backlund, G. Reiter, and A. Rising, "Post-Spin Stretch Improves Mechanical Properties, Reduces Necking, and Reverts Effects of Aging in Biomimetic Artificial Spider Silk Fibers," *ACS Applied Polymer Materials* 6 (2024): 14342–14350.

40. Q. Peng, Y. Zhang, L. Lu, et al., "Recombinant Spider Silk From Aqueous Solutions via a Bio-Inspired Microfluidic Chip," *Scientific Reports* 6 (2016): 36473.

41. A. D. Malay, H. C. Craig, J. Chen, N. A. Oktaviani, and K. Numata, "Complexity of Spider Dragline Silk," *Biomacromolecules* 23 (2022): 1827–1840.

42. L. Y. Yeo, H. C. Chang, P. P. Chan, and J. R. Friend, "Microfluidic Devices for Bioapplications," *Small* 7 (2011): 12–48.

43. J. Chen, A. Tsuchida, A. D. Malay, et al., "Replicating Shear-Mediated Self-Assembly of Spider Silk Through Microfluidics," *Nature Communications* 15 (2024): 527.

44. A. Heidebrecht, L. Eisoldt, J. Diehl, et al., "Biomimetic Fibers Made of Recombinant Spidroins With the Same Toughness as Natural Spider Silk," *Advanced Materials* 27 (2015): 2189–2194.

45. M. Saric and T. Scheibel, "Two-In-One Spider Silk Protein With Combined Mechanical Features in All-Aqueous Spun Fibers," *Biomacromolecules* 24 (2023): 1744–1750.

46. G. Collins, J. Federici, Y. Imura, and L. H. Catalani, "Charge Generation, Charge Transport, and Residual Charge in the Electrospinning of Polymers: A Review of Issues and Complications," *Journal of Applied Physics* 111 (2012): 044701–044701.

47. P. Kiselev and J. Rosell-Llompart, "Highly Aligned Electrospun Nanofibers by Elimination of the Whipping Motion," *Journal of Applied Polymer Science* 125 (2012): 2433–2441.

48. M. Humenik, G. Lang, and T. Scheibel, "Silk Nanofibril Self-Assembly Versus Electrospinning," *Wiley Interdisciplinary Reviews: Nanomedicine and Nanobiotechnology* 10, no. 4 (2018): e1509, https://doi.org/10.1002/wnan.1509.

49. M.-L. Wang, D.-G. Yu, and S. W. A. Bligh, "Progress in Preparing Electrospun Janus Fibers and Their Applications," *Applied Materials Today* 31 (2023): 101766.

50. Z. Lamberger, S. Zainuddin, T. Scheibel, and G. Lang, "Polymeric Janus Fibers," *ChemPlusChem* 88 (2023): e202200371.

51. N. K. Bhardwaj and S. Subhas, "Electrospinning: A Fascinating Fiber Fabrication Technique," *Biotechnology Advances* 28, no. 3 (2010): 325–347, https://doi.org/10.1016/j.biotechadv.2010.01.004.

52. M. Eslamian, M. Khorrami, N. Yi, S. Majd, and M. R. Abidian, "Electrospinning of Highly Aligned Fibers for Drug Delivery Applications," *Journal of Materials Chemistry B* 7 (2019): 224–232.

53. D. Jao, X. Hu, and V. Beachley, "Bioinspired Silk Fiber Spinning System via Automated Track-Drawing," *ACS Applied Bio Materials* 4 (2021): 8192–8204.

54. L. S. Carnell, E. J. Siochi, N. M. Holloway, et al., "Aligned Mats From Electrospun Single Fibers," *Macromolecules* 41 (2008): 5345–5349.

55. J. Yoon, H. S. Yang, B. S. Lee, and W. R. Yu, "Recent Progress in Coaxial Electrospinning: New Parameters, Various Structures, and Wide Applications," *Advanced Materials* 30 (2018): e1704765.

56. P. Rathore and J. D. Schiffman, "Beyond the Single-Nozzle: Coaxial Electrospinning Enables Innovative Nanofiber Chemistries, Geometries, and Applications," *ACS Applied Materials & Interfaces* 13 (2021): 48–66.

57. F. Müller, S. Jokisch, H. Bargel, and T. Scheibel, "Centrifugal Electrospinning Enables the Production of Meshes of Ultrathin Polymer Fibers," *ACS Applied Polymer Materials* 2 (2020): 4360–4367.

58. M. Clark, *Handbook of Textile and Industrial Dyeing: Principles, Processes and Types of Dyes* (Woodhead Publishing, 2011).

59. S. Wu, T. Dong, Y. Li, et al., "State-of-the-Art Review of Advanced Electrospun Nanofiber Yarn-Based Textiles for Biomedical Applications," *Applied Materials Today* 27 (2022): 101473.

60. A. E. Albertson, F. Teulé, W. Weber, J. L. Yarger, and R. V. Lewis, "Effects of Different Post-Spin Stretching Conditions on the Mechanical Properties of Synthetic Spider Silk Fibers," *Journal of the Mechanical Behavior of Biomedical Materials* 29 (2014): 225–234.

61. P. Xiang, S.-S. Wang, M. He, et al., "The In Vitro and In Vivo Biocompatibility Evaluation of Electrospun Recombinant Spider Silk Protein/PCL/Gelatin for Small Caliber Vascular Tissue Engineering Scaffolds," *Colloids and Surfaces B: Biointerfaces* 163 (2018): 19–28.

62. S. Jokisch, M. Neuenfeldt, and T. Scheibel, "Silk-Based Fine Dust Filters for Air Filtration," *Advanced Sustainable Systems* 1 (2017): 1.

63. S. Zainuddin and T. Scheibel, "Continuous Yarn Electrospinning," *Text* 2 (2022): 124–141.

64. A. Koeppel and C. Holland, "Progress and Trends in Artificial Silk Spinning: A Systematic Review," *ACS Biomaterials Science & Engineering* 3 (2017): 226–237.